CHEMISTRY
A EUROPEAN JOURNAL

ChemPubSoc
Europe

DOI: 10.1002/chem.201302600

Angular-Resolved Magnetometry Beyond Triclinic Crystals: Out-of-Equilibrium Studies of Cp*ErCOT Single-Molecule Magnet**

Marie-Emmanuelle Boulon,[a] Giuseppe Cucinotta,[a] Shan-Shan Liu,[b] Shang-Da Jiang,[b] Liviu Ungur,[c] Liviu F. Chibotaru,[c] Song Gao,[b] and Roberta Sessoli*[a]

Abstract: Angular-resolved single-crystal magnetometry is a key tool to characterise lanthanide-based materials with low symmetry, for which conjectures based on idealised geometries can be totally misleading. Unfortunately the technique is strictly successful only for triclinic structures, thus reducing significantly its application. By collecting out-of-equilibrium magnetisation data the technique was extended to the orthorhombic organometallic Cp*ErCOT single-molecule magnet (SMM), thus allowing for the first time the reconstruction of the molecular anisotropy tensor notwithstanding the two molecular orientations in the crystal lattice. The results, flanked by state-of-the-art ab initio calculations, confirmed the expected orientation of the molecular easy axis of magnetisation and thus validated the synthetic strategy based on organometallic complexes of a single lanthanide ion.

Keywords: ab initio calculations · anisotropy · lanthanides · magnetic properties · molecular design

Introduction

Lanthanide-based materials are currently employed in a large variety of applications that range from energy[1] to medicine[2] and catalysis.[3] They play a crucial role in magnetism,[4] thanks to their large number of unpaired electrons and the strong unquenched orbital contribution that characterises 4f electrons. Their employment in molecular magnetism has been constantly on the increase since the discovery of magnetic bistability of molecular origin in a restricted class of polynuclear paramagnetic complexes known as single-molecule magnets (SMMs)[5] and even more rapidly since the observation of the same phenomenon in systems that comprise a single lanthanide ion embedded in two phthalocyaninate rings,[6] $TbPc_2$. These SMMs have been investigated at the single-molecule level by depositing them on metallic and magnetic surfaces,[7] attaching them on carbon nanotubes,[8] or inserting a single molecule in nanogaps,[9] A significant increase in the blocking temperature has instead been achieved by bridging lanthanide ions with N_2^{3-} radicals.[10] The key point to obtain SMM behaviour is the existence of an energy barrier between two orientations of the magnetisation. This can be originated by easy-axis magnetic anisotropy of the system (i.e., Ising anisotropy). In lanthanide-based materials this can be achieved by a rational design of the complex to control the spatial distribution of the ligand negative charges.[11] However, small deviations from uniaxial symmetry are sufficient to induce quantum tunnelling of the magnetisation, which is particularly efficient in lanthanide-based SMMs that comprise a single ion. Different approaches such as employing phthalocyaninate,[6] polyoxometalates,[12] or organometallic sandwich ligands[13] have been developed to obtain axial SMMs, although recent investigations have suggested that relying on idealised symmetry can be misleading, because minor structural features can strongly affect the magnetic anisotropy.[14]

To establish sound magnetostructural correlations, detailed information on the magnetic anisotropy is required.[15] These can be obtained, for instance, by investigating the angular dependence of the magnetisation. However, this approach allows one to measure the sum of all molecular contributions and consequently it can be used to determine the anisotropy axis of the SMM only when molecules in the crystal present a unique orientation of the anisotropy tensor, that is, when related by either translations or inversion centres. Triclinic crystals satisfy this condition but they represent less than one-third of the reported lanthanide complexes. Therefore, until now angular-resolved magnetometry presented limits to the direct definition of the mag-

[a] Dr. M.-E. Boulon, G. Cucinotta, Prof. R. Sessoli
Dipartimento di Chimica Ugo Schiff
Università degli Studi di Firenze
Via della Lastruccia 3-13, 50019 Sesto Fiorentino (Italy)
E-mail: roberta.sessoli@unifi.it

[b] S.-S. Liu, Dr. S.-D. Jiang, Prof. S. Gao
Beijing National Laboratory of Molecular Science
State Key Laboratory of Rare Earth Materials Chemistry and Applications, College of Chemistry and Molecular Engineering
Peking University, Beijing 100871 (P.R. China)

[c] Dr. L. Ungur, Prof. L. F. Chibotaru
Division of Quantum and Physical Chemistry
Department of Chemistry, Katholieke Universiteit Leuven
Celestijnenlaan 200F 3001 Heverlee, Leuven (Belgium)

[**] Cp* = pentamethylcyclopentadiene anion ($C_5Me_5^-$); COT = cyclooctatetraene dianion ($C_8H_8^{2-}$).

Supporting information for this article is available on the WWW under http://dx.doi.org/10.1002/chem.201302600.

netic anisotropy for most lanthanide-based SMMs. We propose here a way to extend single-crystal magnetic investigations to a wider class of molecules beyond those that crystallise in the triclinic system. Although angular-resolved investigations of the hysteretic behaviour of SMMs have been performed in the past, for instance, to provide evidence for the low symmetry of individual Mn_{12}ac clusters due to disorder in the tetragonal crystal structure,[16] a simpler method that directly combines angular dependence of the magnetisation and dynamics data is proposed here to easily access the magnetic anisotropy of SMMs that crystallise with non-collinear orientation. In this category of molecules falls the widely investigated $TbPc_2 \cdot CH_2Cl_2$, as well as the recently reported organometallic SMM Cp*ErCOT,[13a] in which Cp* is the pentamethylcyclopentadiene anion and COT is the cyclooctatetraene dianion.

Cp*ErCOT is of great appeal for fundamental studies on hybrid nanostructures that are of interest for molecular spintronics because it is soluble in most organic solvents and can be evaporated. In the Cp*ErCOT complex, the coordination of a cyclic polyolefin anion with delocalised π electrons was chosen with the purpose of generating a higher local axial symmetry.[13a] As the two rings are tilted by 8°, it is not possible to geometrically define a molecular axis. We therefore decided to investigate its magnetic anisotropy despite the complex crystallising in the orthorhombic space group *Pnma* with two families of almost perpendicular molecules related by a binary axis parallel to *b*. The use of angular-resolved magnetometry in the out-of-equilibrium magnetised state allowed us to separate the contributions that come from the two families of molecules and to compare the detected anisotropy with predictions based on quantum chemical calculations.

Results and Discussion

Single crystals of large dimensions (more than 1 mm length) were grown from a cooled toluene solution (see the Supporting Information). We adapted the previously described procedure[15,17] to perform the measurement of the angular dependence of the susceptibility. As Cp*ErCOT is only stable under an inert atmosphere, the entire sample preparation was carried out in a glovebox, whereas the face indexing and the installation on the rotating system were performed under nitrogen gas flux. In this kind of experiment, usually three orthogonal rotations are performed, but here only two are relevant due to *ac* plane symmetry. The strong air sensitivity of the compound did not allow us to take the time to perfectly align the crystal to perform rotations along the crystallographic axes. We therefore proceeded by embedding the crystal on eicosane on the face of a millimetric Teflon cube, the faces of which were then accurately indexed with crystal *hkl* vectors by using the X-ray diffraction peaks of the single crystal.[15,17a] From here on, the two rotations are labelled as **Rot1**, which was performed along a vector ω_1 nearly perpendicular to *b*, and **Rot2**, which was performed by rotating along a vector ω_2 almost collinear to *b* (see the Supporting Information for an exact definition of ω_1 and ω_2). By rotating the crystal in the magnetic field, we measured the sum of two different contributions that come from the two families of symmetry-related but magnetically non-equivalent molecules.

The angular dependence of the magnetic susceptibility at $T = 10$ K is reported in Figure 1a for the two rotations. **Rot1**

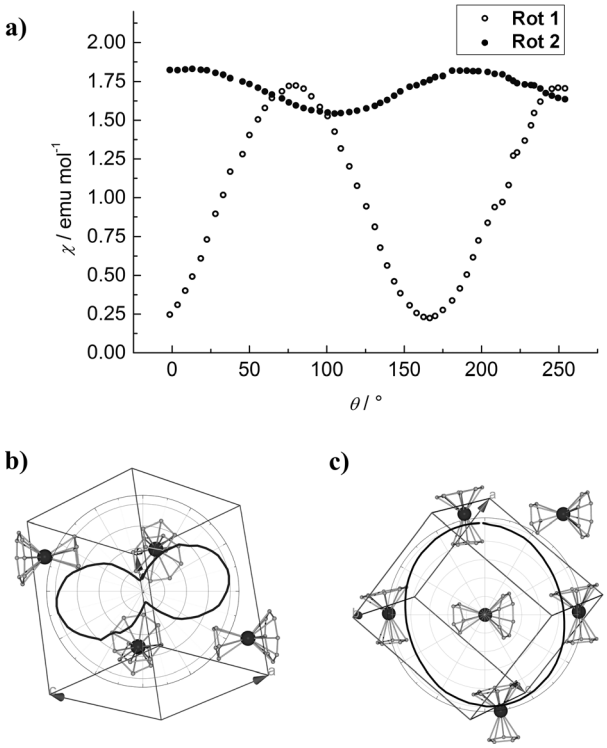

Figure 1. a) Angular dependence of the magnetic susceptibility at 10 K and 1 kOe static field for the rotation along *b* (black dots) and perpendicular to *b* (white dots). b) Polar plot of the measured magnetic susceptibility superimposed over the crystal packing for **Rot1**. c) Polar plot of the measured magnetic susceptibility superimposed over the crystal packing for **Rot2**. Er atoms are represented in dark grey, C in light grey, H are omitted for clarity as well as Me groups on the Cp* ring.

provides evidence that the system possesses a large magnetic anisotropy. By projecting the anisotropy of the magnetic susceptibility on the crystal structure (Figure 1b), we notice that the minimum of the susceptibility is observed when the magnetic field is applied in the equatorial plane (i.e., the plane of the cyclic ligands) of both families of symmetry-related molecules. On the other hand, the maximum corresponds to the case in which the magnetic field is approximately along the pseudosymmetry axis of only one family and perpendicular to the other. We can therefore deduce that at least one direction in the equatorial plane of the sandwich structure is a hard axis of magnetisation. **Rot2** shows a completely different behaviour; the susceptibility is much less anisotropic. In this rotation the field roughly scans the *ac* plane, which corresponds to the symmetry plane of both families of molecules (Figure 1c). Two princi-

pal directions of each molecular anisotropy tensor were therefore probed in the rotation, but with the tensors of the two families related by a glide plane orthogonal to *c*.

The lack of strong anisotropy in **Rot2** can correspond to two limiting cases: the first one is that the system has almost easy-plane anisotropy in the *ac* plane, whereas the sum of two almost perpendicular easy-axis contributions corresponds to the second. In this case the susceptibility follows a $\cos^2\theta$ dependence, with θ being the angle formed by the field with the molecular easy axis (Figure S1 in the Supporting Information), and becomes isotropic if two contributions are tilted by 90°. Even if the latter hypothesis is the most consistent with the quasi-axial symmetry of the complex and its magnetic bistability, any intermediate situations between the limiting cases described above could provide the same observed behaviour. To obtain information independently from any a priori assumption, measurements at low temperature were carried out. Whereas the angular dependence of the magnetisation does not exhibit any particular feature by cooling the temperature in **Rot1** (Figure S2 in the Supporting Information), **Rot2** reveals the appearance of a third maximum below 5 K (Figure 2). As already shown by Gao

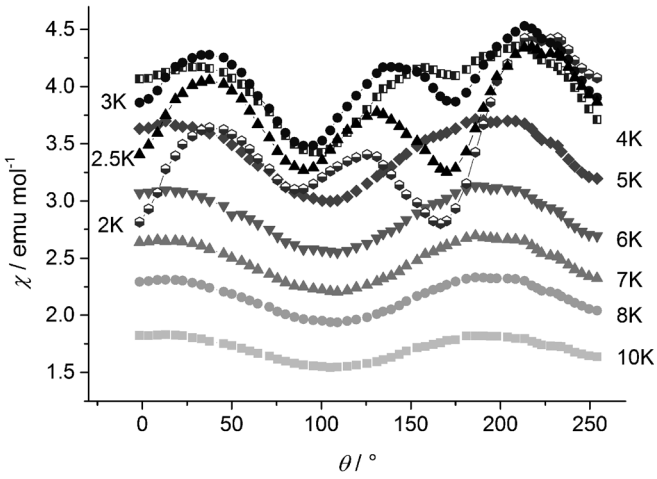

Figure 2. Angular dependence of the magnetic susceptibility at $H=1$ kOe for the rotations (**Rot2**) at various temperatures.

and co-workers[13a,18] the opening of the magnetisation hysteresis loops occurs in Cp*ErCOT below 5 K. If we look for a correlation between the opening of hysteresis loops and the appearance of the third maximum in **Rot2**, the hysteresis curves were measured at 5, 4 and 2 K. We chose the angular position that corresponds to the maxima of susceptibility to record as much signal as possible. Opening of the hysteresis below 5 K was observed for the three investigated angular positions (Figure S3 in the Supporting Information) but only data for $\theta=8.5$, 33 and 37.5° (respectively for $T=5$, 3 and 2 K) are reported in Figure 3. The cycles showed a butterfly shape, which is typical of efficient zero-field quantum tunnelling. The appearance of the third maximum in the angular dependence of the susceptibility seems therefore to correlate with the opening of the hysteresis cycle. However, in

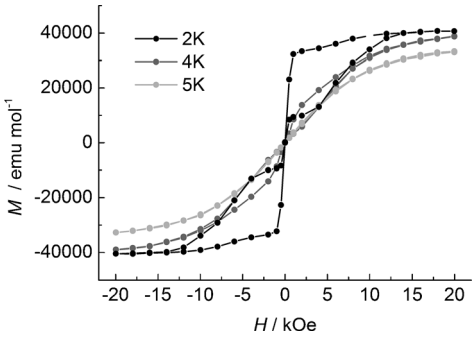

Figure 3. Hysteresis loops recorded at the first maximum of the rotation on a single crystal at 2, 4 and 5 K. Hysteresis loops at other angular positions are presented in Figure S3 of the Supporting Information.

our experiments the intensity of the magnetic field, $H=1$ kOe, was kept constant during the rotation and only its projection along the molecular axes varied. The observation of a hysteresis-related behaviour is therefore only compatible with an intrinsic, or molecular, magnetic anisotropy in the probed crystallographic plane. Below 5 K, due to the slow relaxation, the magnetisation of each molecule cannot reach the equilibrium value after each change of the orientation of the magnetic field and its contribution to the susceptibility of the crystal deviates from the $\cos^2\theta$ behaviour. The averaging of the contributions of the two families of symmetry-related molecules, which characterises the smooth behaviour at $T=10$ K, is therefore lost in the hysteretic regime.

To confirm this hypothesis, **Rot2** was repeated on a new crystal using two different timescales (this time the rotation axis deviated from the *b* axis by only 2°). First, the shortest delay allowed by our experimental setup ($\approx$50 s) was applied between two successive angular positions. In the second case a delay equal to 2300 s was introduced between each step of the rotation and the data acquisition to let the system relax to equilibrium. The results obtained at $T=4$ K (Figure 4a) fully support our conjecture. The measurements performed with the long delay (Figure 4a, empty circles) do not show the three-peak profile that characterises the system out of equilibrium (black dots) but present a behaviour similar to the one obtained above 5 K, when hysteresis effects are not present. Data collected with a long delay were therefore simulated by summing up (pink line in Figure 4a) the two square cosine functions (dashed green and cyan lines) of two easy-axis magnetic centres with an amplitude of 5.160(4) emu mol^{-1}, separated by an angle of 94.60(6)°. The same two contributions were then used to simulate the out-of-equilibrium data obtained with the shortest delay assuming an exponential decay. The behaviour of the magnetisation $M(\theta)$ at time, *t*, was fitted point-by-point by using the exponential relation [Eq. (1)]:

$$M(\theta,i) = M_{eq}(\theta,i) + \Delta M_i e^{-\frac{\sigma_i}{\tau(H)}} \quad (1)$$

in which M_{eq} is the value of magnetisation at equilibrium (obtained for each θ from the long-delay measurements), σ_i

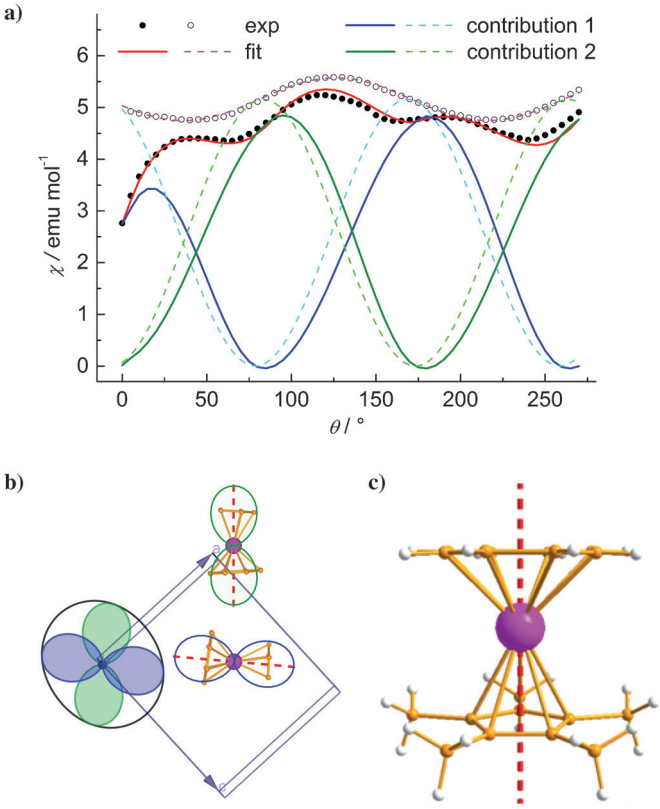

Figure 4. a) Fit (red and pink lines) of the experimental angular dependence of the magnetic susceptibility measured with short (●) and long (○) time delays. The two deconvoluted contributions are shown in blue and green as dashed and solid curves for equilibrium and out of equilibrium, respectively. b) Polar plot of the two contributions (same colour code as above) and of their sum (black line) superimposed over the crystal cell content view along *b* and to the same quantities obtained from ab initio calculations. c) View of the orientation of the calculated easy axis of magnetisation (red broken line).

is the time elapsed between measurement i and the subsequent $i+1$ during which the system tends toward equilibrium (assuming that the time of the rotations between two positions is negligible); ΔM_i measures how far from equilibrium the system is at every change of field and $\tau(H)$ is the relaxation time. A better agreement was obtained by assuming that $\tau(H)$ depends on the variation of the field according to an increase or decrease through a linear relationship composed of a magnetic-field-independent component (τ_0) and by a term linearly dependent on the projection of H along the easy axis according to Equation (2):

$$\tau = \tau_0 + AH[\cos(\theta)] \qquad (2)$$

The difference between increasing and decreasing field situations is expressed through the A constant, which in the best-fit simulation assumes two values: $A_{inc} = 0.210(5)\ s\,Oe^{-1}$ and $A_{dec} = 0.140(5)\ s\,Oe^{-1}$, for increasing and decreasing field projection, respectively, whereas $\tau_0 = 105(5)$ s. In Figure 4a the red line represents the sum of the two out-of-equilibrium contributions (solid cyan and green lines) obtained with the best-fit parameters mentioned above. Positive A values reflect the slowing down of the magnetic relaxation when a weak magnetic field is applied due to suppression of the tunnel mechanism. Different values observed upon decreasing or increasing the longitudinal component of the magnetic field during the rotation is not unexpected, since the initial magnetisation state of the material affects also the tunnelling mechanism by modifying the local magnetic field.[19]

Measurements at $T = 3.5$ K were also performed (Figures S4 and S5 in the Supporting Information) but not at lower temperatures because protracted times are needed to reach equilibrium. Although the few points available do not allow one to extract the temperature dependence of the relaxation parameters, our analysis allowed us to deconvolute the contributions of each family of strongly anisotropic molecules from a quasi-isotropic behaviour of the crystal at thermodynamic equilibrium (Figure 4b). A reasonable simulation of the out-of-equilibrium anisotropy can only be achieved if two almost orthogonal Ising-like contributions are present, but it is not possible to associate unambiguously each contribution to one particular family of symmetry-related molecules. Ab initio calculations were performed since the molecular easy axis of magnetisation of the Cp*ErCOT complex can therefore be either along each pseudosymmetry axis or orthogonal to it.

Calculations on the basis of the relativistic self-consistent field CASSCF-RASSI-SO/SINGLE_ANISO as implemented in the MOLCAS code[20] have proven to be a reliable tool for the description of magnetic anisotropy of lanthanide-based compounds.[15,17b,21] The experimental structure of the Cp*ErCOT determined at 120 K showed that the COT ligand is disordered over two positions with equal populations. Ab initio calculations (see the Supporting Information for details and results) on the basis of these geometries revealed that the ground Kramers doublet is expected to be strongly axial, with transversal effective g factors $g_x, g_y < 10^{-3}$, and g_z approaching the value of 18 expected for the ground doublet of a pure Ising $J = 15/2$ state with $g_J = 6/5$ (Table 1). Calculations also showed that the easy axis, which corresponds to g_z orientation, lies perpendicularly to the average of the planes of the two rings of COT and Cp* ligands (Figure 4c and Figure S6 in the Supporting Information). The high degree of magnetic axiality of the ground state of both conformers ensures their capability to block the magnetisation.

Table 1. Principal values of the g tensors of the ground doublet (assuming an effective spin of $^1/_2$) and the energy gap between the ground and the first excited doublets obtained from ab initio calculations.[a]

	Experimental structure at 120 K		DFT-optimised structure	
	1	**2**	**1**	**2**
g_x	0.00062	0.00057	0.00000	0.00002
g_y	0.00086	0.00085	0.00005	0.00002
g_z	17.947	17.939	17.945	17.944
ΔE [cm^{-1}]	84.8	115.9	134.9	135.2

[a] The experimental structures of the two conformers that differ in the position of the COT ligand were used in the calculation as well as starting points for a DFT optimisation of the geometry.

In Figure 4b the calculated angular plot of the dependence of the susceptibility (averaged over the two conformers), shown as the green and blue lines superimposed over the corresponding molecules, is compared with the ones used to reproduce the experimental susceptibility of the crystal, represented by the shadowed angular plot on the corner of the cell (see also Figures S7 and S8 in the Supporting Information). The excellent agreement confirms the reliability of the extraction of the molecular anisotropy from crystal data.

The calculated energy gaps with the first excited Kramers doublet on the two conformers, 84.8 and 115.9 cm^{-1} (Table 1 and Table S1 in the Supporting Information), are lower than the activation energies, 137 and 224 cm^{-1} extracted from alternating current (ac) susceptibility data.[13a] Although the capability of this theoretical approach to reproduce the orientation of the anisotropy tensors is well documented, the comparison between calculated energy levels and independent estimations of them, for example, through luminescence spectra, are still scarce.

One reason for the observed discrepancy could be that the experimental geometry used at 120 K might not represent the low-temperature geometry accurately enough. Optimisation of the geometry of the two conformers at the DFT level without taking into account the intermolecular interactions (see the Supporting Information) did in fact yield a single structure. By using these optimised geometries the anisotropies of the ground Kramers doublets—particularly the directions of corresponding anisotropy axes—remain practically unchanged with respect to previous calculations (Tables S1 and S3 in the Supporting Information). However, the first excitation energy is now obtained at 135 cm^{-1}, which closely matches the lower activation energy. We expect that a more accurate geometry optimisation that takes into account the intermolecular interaction will result in distinct geometries for the two conformers and a closer reproduction of the second activation energy.

Conclusion

In conclusion, we successfully determined the magnetic anisotropy of the Cp*ErCOT SMM by performing measurements on single-crystal samples, notwithstanding the two molecular orientations in the crystal lattice. Angular-resolved magnetic measurements under in- and out-of-equilibrium conditions allowed us to ascertain that the molecule possesses an easy axis of magnetisation. The complex was designed to optimise the energy barrier by creating axial symmetry around the metal ion and the hypothesis of axial magnetic anisotropy parallel to the molecular main direction is here confirmed by means of experiments and ab initio calculations.

The original experimental protocol described herein to extract information on the magnetic anisotropy of SMMs, even when more than one orientation is present in the crystal lattice, is of great relevance to develop a rational design of magnetic materials with increased anisotropy, as well as to pick out the most promising molecules to design hybrid nanostructures of interest in molecular spintronics.

Experimental Section

The compound was synthesised following the previously described method with slight modifications.[13a,18,22] Prismatic pink crystals suitable for X-ray diffraction and for the single-crystal magnetic measurements were obtained by crystallisation from toluene solution at −30 °C for several days in a glovebox. Crystals glued onto a Teflon cube were indexed by X-ray diffraction using an Oxford Diffraction Xcalibur3 diffractometer and mounted on a horizontal rotating system from Quantum Design for angular-dependent magnetometry studies. Magnetic measurements were performed using a Quantum Design MPMS Squid magnetometer. All calculations have been performed with the MOLCAS 7.8 program package and were of the CASSCF/RASSI/SINGLE_ANISO type.

Acknowledgements

Financial support from the European Research Council through the Advanced Grant "MolNanoMas" (project no. 267746), from the Italian MIUR, through the FIRB project RBAP117RWN, from INPAC, from the Methusalem programs at KU Leuven, from the Chinese NSFC (90922033) and MOST (2013CB933401) is acknowledged. L.U. is a postdoc of the Flemish Science Foundation (FWO).

[1] a) F. Wang, R. Deng, J. Wang, Q. Wang, Y. Han, H. Zhu, X. Chen, X. Liu, *Nat. Mater.* **2011**, *10*, 968–973; b) X. Huang, S. Han, W. Huang, X. Liu, *Chem. Soc. Rev.* **2013**, *42*, 173–201.
[2] J. Zhang, Y. Li, X. Hao, Q. Zhang, K. Yang, L. Li, L. Ma, S. Wang, X. Li, *Mini-Rev. Med. Chem.* **2011**, *11*, 678–694.
[3] W. Qin, D. Zhang, D. Zhao, L. Wang, K. Zheng, *Chem. Commun.* **2010**, *46*, 2304–2306.
[4] a) J. M. D. Coey, Oxford University Press, Oxford, **1996**; b) J. Jensen, A. R. Mackintosh, *Rare Earth Magnetism: Structures and Excitations*, Clarendon, Oxford, **1991**.
[5] a) D. Gatteschi, R. Sessoli, J. Villain, *Molecular nanomagnets*, Oxford University Press, Oxford, **2006**; b) G. Christou, D. Gatteschi, D. N. Hendrickson, R. Sessoli, *Mater. Res. Bull.* **2000**, *35*, 66–71.
[6] N. Ishikawa, M. Sugita, T. Ishikawa, S. Koshihara, Y. Kaizu, *J. Am. Chem. Soc.* **2003**, *125*, 8694–8695.
[7] a) T. Komeda, H. Isshiki, J. Liu, Y.-F. Zhang, N. Lorente, K. Katoh, B. K. Breedlove, M. Yamashita, *Nat. Commun.* **2011**, *2*, 217; b) A. L. Rizzini, C. Krull, T. Balashov, J. J. Kavich, A. Mugarza, P. S. Miedema, P. K. Thakur, V. Sessi, S. Klyatskaya, M. Ruben, S. Stepanow, P. Gambardella, *Phys. Rev. Lett.* **2011**, *107*, 177205; c) L. Vitali, S. Fabris, A. M. Conte, S. Brink, M. Ruben, S. Baroni, K. Kern, *Nano Lett.* **2008**, *8*, 3364–3368; d) J. Schwöbel, Y. Fu, J. Brede, A. Dilullo, G. Hoffmann, S. Klyatskaya, M. Ruben, R. Wiesendanger, *Nat. Commun.* **2012**, *3*, 953.
[8] a) M. Urdampilleta, S. Klyatskaya, J. P. Cleuziou, M. Ruben, W. Wernsdorfer, *Nat. Mater.* **2011**, *10*, 502–506; b) M. Ganzhorn, S. Klyatskaya, M. Ruben, W. Wernsdorfer, *Nat. Nano* **2013**, *8*, 165–169.
[9] R. Vincent, S. Klyatskaya, M. Ruben, W. Wernsdorfer, F. Balestro, *Nature* **2012**, *488*, 357–360.
[10] a) J. D. Rinehart, M. Fang, W. J. Evans, J. R. Long, *J. Am. Chem. Soc.* **2011**, *133*, 14236–14239; b) J. D. Rinehart, M. Fang, W. J. Evans, J. R. Long, *Nat. Chem.* **2011**, *3*, 538–542.
[11] a) J. D. Rinehart, J. R. Long, *Chem. Sci.* **2011**, *2*, 2078–2085; b) J. J. Baldoví, S. Cardona-Serra, J. M. Clemente-Juan, E. Coronado, A. Gaita-Ariño, A. Palii, *Inorg. Chem.* **2012**, *51*, 12565–12574.

[12] M. A. AlDamen, J. M. Clemente-Juan, E. Coronado, C. Marti-Gastaldo, A. Gaita-Arino, *J. Am. Chem. Soc.* **2008**, *130*, 8874–8875.
[13] a) S.-D. Jiang, B.-W. Wang, H.-L. Sun, Z.-M. Wang, S. Gao, *J. Am. Chem. Soc.* **2011**, *133*, 4730–4733; b) M. Jeletic, P.-H. Lin, J. J. Le Roy, I. Korobkov, S. I. Gorelsky, M. Murugesu, *J. Am. Chem. Soc.* **2011**, *133*, 19286–19289.
[14] G. Cucinotta, M. Perfetti, J. Luzon, M. Etienne, P. E. Car, A. Caneschi, G. Calvez, K. Bernot, R. Sessoli, *Angew. Chem.* **2012**, *124*, 1638–1642; *Angew. Chem. Int. Ed.* **2012**, *51*, 1606–1610.
[15] J. Luzon, R. Sessoli, *Dalton Trans.* **2012**, *41*, 13556–13567.
[16] E. Del Barco, A. D. Kent, E. M. Rumberger, D. N. Hendrickson, G. Christou, *Phys. Rev. Lett.* **2003**, *91*, 047203.
[17] a) I. J. Hewitt, J. Tang, N. T. Madhu, C. E. Anson, Y. Lan, J. Luzon, M. Etienne, R. Sessoli, A. K. Powell, *Angew. Chem.* **2010**, *122*, 6496–6500; *Angew. Chem. Int. Ed.* **2010**, *49*, 6352–6356; b) M.-E. Boulon, G. Cucinotta, J. Luzon, C. Degl′innocenti, M. Perfetti, K. Bernot, G. Calvez, A. Caneschi, R. Sessoli, *Angew. Chem.* **2013**, *125*, 368–372; *Angew. Chem. Int. Ed.* **2013**, *52*, 350–354.
[18] S.-D. Jiang, S.-S. Liu, L.-N. Zhou, B.-W. Wang, Z.-M. Wang, S. Gao, *Inorg. Chem.* **2012**, *51*, 3079–3087.
[19] a) W. Wernsdorfer, T. Ohm, C. Sangregorio, R. Sessoli, D. Mailly, C. Paulsen, *Phys. Rev. Lett.* **1999**, *82*, 3903–3906; b) T. Ohm, C. Sangregorio, C. Paulsen, *Eur. Phys. J. B* **1998**, *6*, 195–199; c) A. Cuccoli, A. Fort, A. Rettori, E. Adam, J. Villain, *Eur. Phys. J. B* **1999**, *12*, 39–46.
[20] a) F. Aquilante, L. De Vico, N. Ferré, G. Ghigo, P.-å. Malmqvist, P. Neogrády, T. B. Pedersen, M. Pitoňák, M. Reiher, B. O. Roos, L. Serrano-Andrés, M. Urban, V. Veryazov, R. Lindh, *J. Comput. Chem.* **2010**, *31*, 224–247; b) G. Karlstrom, R. Lindh, P. A. Malmqvist, B. O. Roos, U. Ryde, V. Veryazov, P. O. Widmark, M. Cossi, B. Schimmelpfennig, P. Neogrady, L. Seijo, *Comput. Mater. Sci.* **2003**, *28*, 222–239; c) L. F. Chibotaru, L. Ungur, *J. Chem. Phys.* **2012**, *137*, 064112.
[21] a) K. Bernot, J. Luzon, L. Bogani, M. Etienne, C. Sangregorio, M. Shanmugam, A. Caneschi, R. Sessoli, D. Gatteschi, *J. Am. Chem. Soc.* **2009**, *131*, 5573–5579; b) K. Bernot, J. Luzon, A. Caneschi, D. Gatteschi, R. Sessoli, L. Bogani, A. Vindigni, A. Rettori, M. G. Pini, *Phys. Rev. B* **2009**, *79*, 134419; c) L. F. Chibotaru, L. Ungur, A. Soncini, *Angew. Chem.* **2008**, *120*, 4194–4197; *Angew. Chem. Int. Ed.* **2008**, *47*, 4126–4129; d) L. Ungur, S. K. Langley, T. N. Hooper, B. Moubaraki, E. K. Brechin, K. S. Murray, L. F. Chibotaru, *J. Am. Chem. Soc.* **2012**, *134*, 18554–18557; e) Y.-X. Wang, W. Shi, H. Li, Y. Song, L. Fang, Y. Lan, A. K. Powell, W. Wernsdorfer, L. Ungur, L. F. Chibotaru, M. Shen, P. Cheng, *Chem. Sci.* **2012**, *3*, 3366–3370.
[22] H. Schumann, R. D. Kohn, F. W. Reier, A. Dietrich, J. Pickardt, *Organometallics* **1989**, *8*, 1388–1392.

Received: July 4, 2013
Published online: September 3, 2013

